Delft University of Technology

Shear stop criteria for reinforced concrete slab strips

Zarate Garnica, G. I. ; Lantsoght, E. O.L.; Yang, Y.; Hendriks, M. A.N.

Important note
To cite this publication, please use the final published version (if applicable).
Please check the document version above.

Shear stop criteria for reinforced concrete slab strips

G.I. Zarate Garnica
Delft University of Technology, Delft, The Netherlands
Ney & Partners, Delft, The Netherlands

E.O.L. Lantsoght
Delft University of Technology, Delft, The Netherlands
Universidad San Francisco de Quito, Quito, Ecuador

Y. Yang
Delft University of Technology, Delft, The Netherlands

M.A.N. Hendriks
Delft University of Technology, Delft, The Netherlands
NTNU, Norway

ABSTRACT: Proof load testing for assessment can involve a large risk due to the high loads. Stop criteria can reduce this risk. Stop criteria are necessary for shear, which is a brittle failure mode. This paper describes the development of shear stop criteria for slab strips. The shear stop criteria are developed by combining theoretical concepts related to cracking, as well the relationship between bending- and shear-critical regions, along with insights from the Critical Shear Crack Theory and the Critical Shear Displacement Theory. The shear stop criteria are validated with fourteen beam tests. The result is a set of shear stop criteria in a "traffic light system" with a green light level related to serviceability, and yellow and red light related to the ultimate limit state for shear. These stop criteria serve as the basis for a global approach for proof load testing of reinforced concrete bridges.

1 INTRODUCTION

Proof load testing for assessment has gained recognition in the past years as a promising method for bridges for which capacity reserves are expected that cannot be demonstrated with an analytical assessment (Alampalli et al., 2021; Lantsoght, 2023). During a proof load test, a load representative of the factored live load is applied to the bridge. These high loads imply high risks. Therefore, stop criteria are used. Stop criteria are thresholds to the measured responses of the bridge. Once these thresholds are reached, the proof load test should be stopped and further loading is not allowed, as it could result in irreversible damage or potentially even collapse of the bridge.

In the Netherlands, a large number of reinforced concrete slab bridges require assessment, and some of these are good candidates for proof load testing (Lantsoght et al., 2017). However, to come to a wide adoption of the practice of proof load testing for assessment of existing reinforced concrete slab bridges, stop criteria for shear are necessary, as a large number of the existing reinforced concrete slab bridges are found to be shear-critical upon an analytical assessment (Lantsoght et al., 2014).

Theoretically derived stop criteria for flexure are available and validated (Lantsoght et al., 2019). For shear, stop criteria have been proposed based on a small number of experiments (Lantsoght et al., 2018; Yang et al., 2018), but more profound theoretical research was deemed necessary in combination with experiments. The current research on shear stop criteria consists of two steps: 1) theoretically deriving shear stop criteria for reinforced concrete slab strips and validating these criteria with experiments on beams without stirrups, and 2) extending these stop criteria to

slabs and validating these stop criteria on straight and skewed slabs. This paper reports the findings of the first stage.

2 THEORETICAL STOP CRITERIA FOR SHEAR

2.1 *Indicator based on simplified aggregate interlock expression*

Aggregate interlock is one of the main shear-carrying mechanisms. A stop criterion based on aggregate interlock should be linked to a measurable parameter. Crack width is considered as the most suitable measurable parameter to link to aggregate interlock. For the stop criterion, the simplified aggregate expression of the Critical Shear Displacement Theory, CSDT, (Yang et al., 2016) is used. This theory leans on the critical shear displacement Δ, which is difficult to measure during a proof load test. Therefore, a proposal that is based on the crack width w at the level of the tension steel and the acting shear stress τ at the cracked section has been proposed (Yang et al., 2018). Moreover, it is assumed that the aggregate interlock capacity V_{ai} can be taken as a lower bound for the shear capacity V. As a result, the shear capacity expression becomes the expression of the aggregate interlock capacity:

$$V = f_c^{0.56} s_{cr} b \frac{0.03}{w - 0.01} \left(-978\Delta^2 + 85\Delta - 0.27\right) \tag{1}$$

In Eq. (1), f_c is the concrete compressive strength, s_{cr} is the height of a fully developed crack, b is the member width, w is the nominal crack width at the level of the steel reinforcement, and Δ is the shear displacement. Rearranging terms so that all measurable parameters in a proof load test are on the left-hand side of the equation and replacing the shear displacement Δ by the critical shear displacement Δ_{cr} results in:

$$V(w - 0.01) = 0.03 f_c^{0.56} s_{cr} b \left(-978\Delta_{cr}^2 + 85\Delta_{cr} - 0.27\right) \tag{2}$$

with the critical shear displacement Δ_{cr} as:

$$\Delta_{cr} = \frac{25 d_l}{30610 \phi_{eq}} + 0.0022 \leq 0.025 \tag{3}$$

and the equivalent rebar diameter ϕ_{eq} can be determined as:

$$\phi_{eq} = \frac{\Sigma \phi_i^2}{\Sigma \phi_i} \tag{4}$$

The height of the fully developed crack can be determined as:

$$s_{cr} = \left(1 + \rho n - \sqrt{\rho n + (\rho n)^2}\right) d_l \tag{5}$$

with ρ the reinforcement ratio, n the ratio between the Young's modulus of the steel and the Young's modulus of the concrete, and d_l the effective depth to the longitudinal reinforcement. The lefthand side of Eq. (2) can be simplified into the shear indicator I_{CSDT} relating the shear stress τ and nominal crack width w as follows:

$$I_{CSDT} = \frac{V(w - 0.01)}{bs} \approx \frac{V(w - 0.01)}{bd} = \tau(w - 0.01) \tag{6}$$

The critical shear indicator $I_{s,cr}$ then becomes:

$$I_{CSDT,cr} = 0.03 f_c^{0.56} \frac{s_{cr}}{d} \left(-978\Delta_{cr}^2 + 85\Delta_{cr} - 0.27 \right) \tag{7}$$

with Δ_{cr} from Eq. (3) and s_{cr} from Eq. (5).

2.2 Indicator based on Critical Shear Crack Theory

In the Critical Shear Crack Theory, CSCT, (Muttoni & Fernández Ruiz, 2008), the shear strength depends on the crack width and roughness of a critical shear crack (expressed as a function of the maximum aggregate size d_g). In other words, the CSCT considers aggregate interlock as the main shear-carrying mechanism. One of the main assumptions in the theory is that the critical crack width w can be taken as proportional to the multiplication of longitudinal strain ε_x and indication of crack spacing d at a control depth of $0.6d$ from the top fiber. Using these considerations, the shear strength V_R is expressed as:

$$\frac{V_R}{bd\sqrt{f_c}} = \frac{1}{6} \frac{2}{1 + 120 \frac{\varepsilon_x d}{16 + d_g}} \tag{8}$$

with f_c the concrete compressive strength (in MPa), b the width, d the effective depth, ε_x the longitudinal strain at the control depth derived from the bending moment demand in the critical section, and d_g the maximum aggregate size in mm. Replacing the shear resistance V_R by the sectional shear V, an indicator can be derived with f_c in MPa and d_g in mm:

$$
\begin{aligned}
I_{CSCT} &= \frac{V}{bd\sqrt{f_c}} = \frac{1}{6} \frac{2}{1 + 120\frac{\varepsilon_x d}{16 + d_g}} = \frac{1}{3} \frac{1}{1 + 120\frac{w}{d_g}} \\
I_{CSCT} &= \frac{V}{bd} \left(1 + 120\frac{w}{d_g} \right) = \tau \left(1 + 120\frac{w}{d_g} \right) \leq \frac{\sqrt{f_c}}{3}
\end{aligned}
\tag{9}
$$

In this expression, the measurable parameters are V (as a function of the applied load) and ε_x, which can be derived from the strain at the level of the tension reinforcement and assuming a linear strain distribution as:

$$\varepsilon_x = \frac{0.6d - c}{d - c} \varepsilon_{x,rebar} \tag{10}$$

with d the effective depth and c the height of the compression zone.

2.3 SLS crack width limit

In addition to the considerations, the crack width limitation from the serviceability limit state (SLS) as prescribed by NEN EN 1992-1-1:2005 (CEN, 2005) is studied. The limiting crack width is a function of the exposure class. For reinforced concrete bridges, the SLS limit for crack width is $w_{SLS} = 0.3$ mm. Using the consideration from the previous section, the average crack width w_{avg} can be determined, and compared to the SLS limit as:

$$w_{avg} = \frac{\varepsilon_{c,average} l_g}{n_{cr}} \leq 0.3mm \tag{11}$$

The number of cracks n_{cr} represents the average number of cracks within the gauge length l_g. The difference between the crack spacing between major cracks and secondary cracks at the reinforcement level is considered using a factor of 0.5, resulting in:

$$n_{cr} = \frac{l_g}{0.5 l_{crm}} \qquad (12)$$

with l_{crm} the average crack spacing.

An indicator of the Serviceability Limit State (SLS) is crucial as it serves as a signal for potential repairs after proof loading. Exceeding the SLS limit state can cause limited damage, however, the crack width is restricted so that it will not impair the proper functioning or durability of the structure.

3 EXPERIMENTS

Slab strips of 10 m length × 0.3 m width, and with heights of 500, 800 and 1200 mm were tested to validate the proposed shear stop criteria (Koekkoek & Yang, 2016; Yang, 2021). The slab strips were simply supported and subjected to a single concentrated load. The span length was 9 m, and the distance between the load and the support varied among the experiments. Only one experiment was carried out per beam. The load was applied with a hydraulic jack in displacement-controlled way with a loading speed of 0.02 mm/s. The load was increased stepwise until failure. Figure 1 shows the test setup used in these experiments.

The concrete class was C65/80. The reinforcement consisted of ribbed bars with f_{ym} = 550 MPa. Figure 2 shows the reinforcement layout in the beams. It can be seen that one span is provided with stirrups, to avoid an unexpected failure mode.

Table 1 gives an overview of the parameters of the fourteen selected experiments. The table reports the cube concrete compressive strength $f_{c,cube}$, the rebar configuration, the reinforcement ratio ρ_l, the shear span a, the effective depth to the longitudinal reinforcement d_l and the shear span to depth ratio a/d_l. The naming system of the specimen relates to H for high members, the reinforcement ratio (roughly), and the last digit refers to the number of the identical specimen. The table also includes the test results as P_u, which refers to the load level at which the specimen failed in shear, or for the case of the specimens with low a/d, the load at which the critical shear crack opens.
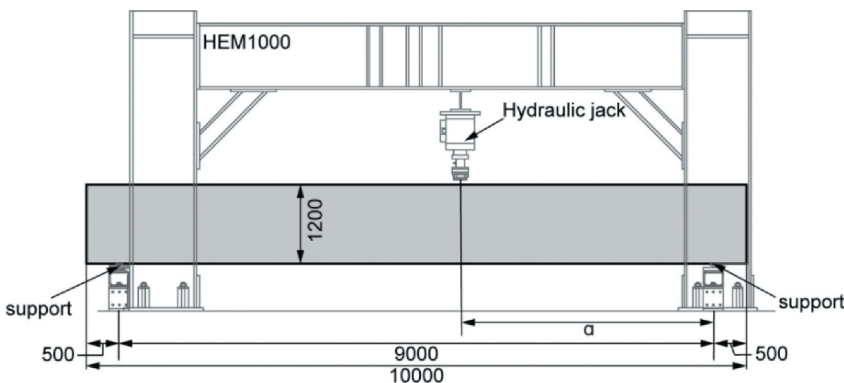

Figure 1. Sketch of test setup. Units in [mm].

The instrumentation on the specimens consisted of traditional sensors such as linear variable differential transformers (LVDTs), laser triangulation sensors (lasers), and the load cell at the hydraulic jack. The structural responses that were measured are deformations in horizontal and vertical direction with the LVDTs as well as deflection under the concentrated load with the lasers. The load cell is sued to report the applied load. Moreover, two-dimensional digital image correlation (2D DIC) is used to monitor the crack pattern and the full displacement field. The displacement field is obtained by using the MatchID (MatchID, 2022) software, as
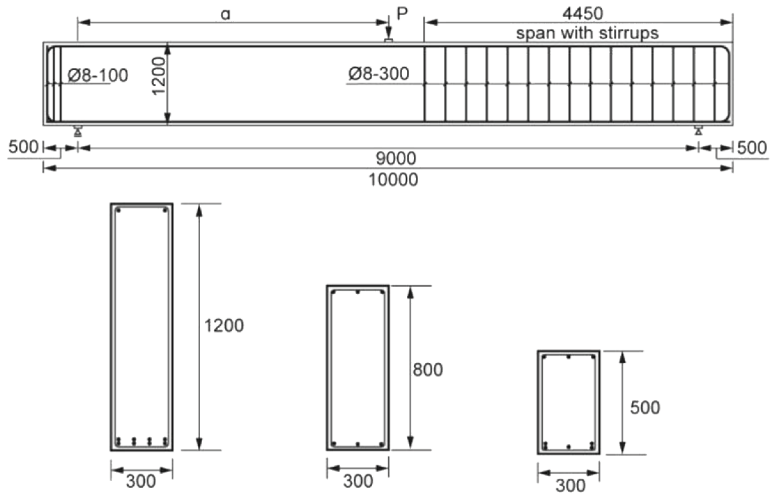
Figure 2. Reinforcement layout of the tested beams. Units in [mm].

Table 1. Parameters of experiments.

Test name	$f_{c,cube}$ (MPa)	Rebar	ρ_l (%)	a (mm)	d_l (mm)	$\lambda=a/d_l$	P_u
H602	86	4Ø25 R	0.57	4500	1158	3.89	306
H401	81	3Ø25 R	0.42	4500	1158	3.89	264
H403	82	3Ø25 R	0.42	4500	1158	3.89	350
H404	82	3Ø25 R	0.42	4000	1158	3.45	269
H121	84	8Ø25 R	1.14	3000	1145	2.62	341
B501A1	81	5Ø20 R	1.15	2500	455	5.5	277
B501B1	76	5Ø20 R	1.15	1500	455	3.3	210
B502B1	77	3Ø20 R	0.68	1750	455	3.8	155
E801A1*	84	3Ø25 R	0.64	2000	770	2.6	213
E801B1	91	3Ø25 R	0.64	2000	770	2.6	205
E802A1	76	6Ø20 R	0.83	2000	740	2.7	219
E802B1*	76	6Ø20 R	0.83	2000	740	2.7	270
E803A1	83	6Ø20 R	0.82	3500	760	4.6	279
E803B1	83	6Ø20R	0.82	3500	760	4.6	308

R for ribbed bars
* specimens with $P_u = P_{cr}$ (load level at which the critical shear crack opened)

well as a Matlab (The Mathworks, 2019) script to obtain the crack pattern, the crack kinematics, and the average strain measurements. The crack pattern and crack kinematics are obtained using the automated detection and crack measurement (ACDM) software (Gehri et al., 2020).

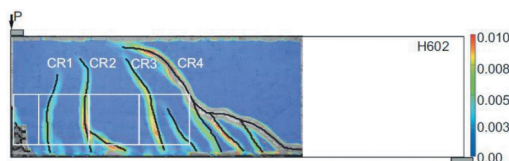Figure 3 shows the crack numbering and crack width determination as applied to H602.

Figure 3. Numbering of cracks, as applied to H602.

4 COMPARISON BETWEEN EXPERIMENTS AND STOP CRITERIA

In order to simulate a real-world measurement of a proof load test, in which the location of the critical cross-section is not known beforehand. The stop criteria are determined at a series of cross-sections of the listed beams along the longitudinal axis. Here the value of crack width or longitudinal strain of a given cross section is determined by a virtual LVDT obtained from the DIC results. The load level when the stop criterion at a given cross-section is reached is noted as P_{ind}. The value of P_{ind} is compared to the measured shear load when shear failure (P_{cr}) is obtained from the test. In general, the ratio between P_{ind}/P_{cr} and M/Vd follows a parabolic trend, see for example Figure 4. In the figure, the factor $\lambda=a/d_l$ for each specimen is given in parenthesis. Overall, the stop criteria related to the shear theories were reached closer to failure in the regions with $M/Vd < 2$. In the region near the loading point between $1d$ and $0.5d$, where the M/Vd is the largest, this corresponds to the area influenced by the largest bending moments and the crack opening and the stop criteria were reached first. This is in line with the model described in CSDT, that a cracked section with smaller M/Vd tends to be more difficult to reach shear failure.

To facilitate the comparison between the various beam experiments with different a/d_l, the M/Vd ratio was normalized by the factor $\lambda= a/d_l$, as shown in Figure 5. This normalization allowed the identification of two main regions: 1) the region corresponding to l_{crm} from the support (larger M/Vd ratios) where the shear resistance is mainly influenced by the crack opening, and 2) the region with the lowest M/Vd which corresponds to shear failure, and where the shear resistance is governed by the shear displacement and the inclination of the cracks.

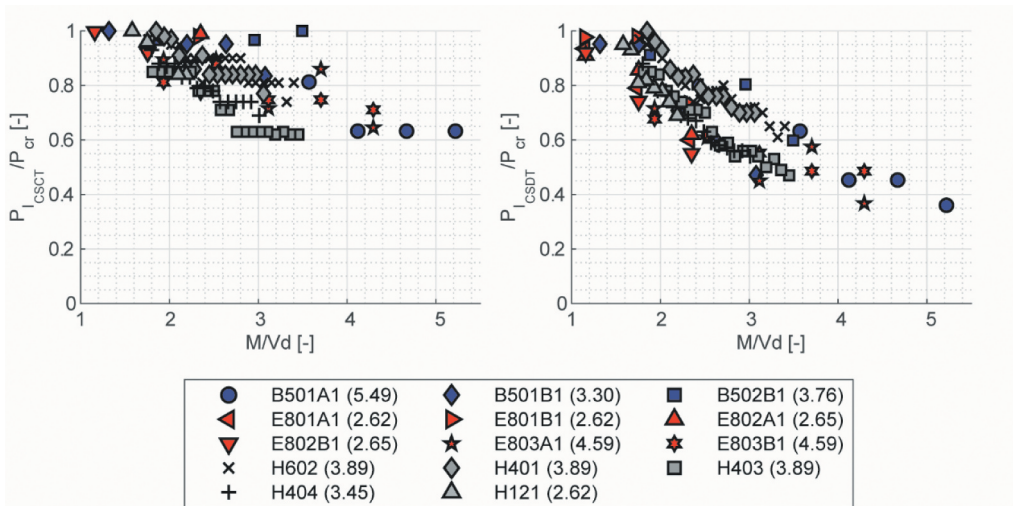|					
●	B501A1 (5.49)	◆	B501B1 (3.30)	■	B502B1 (3.76)
◀	E801A1 (2.62)	▶	E801B1 (2.62)	▲	E802A1 (2.65)
▼	E802B1 (2.65)	★	E803A1 (4.59)	✶	E803B1 (4.59)
✕	H602 (3.89)	◇	H401 (3.89)	▢	H403 (3.89)
+	H404 (3.45)	△	H121 (2.62)		

Figure 4.   Results of the indicator based on the Critical Shear Crack theory and the Critical Shear Displacement Theory as a function of M/Vd.

The summary of the results of the comparison between the stop criteria and the measurements, subdivided into these regions can be found in Table 2. The results of large M/Vd include the measurements between $0.8<M/Vd\times(1/\lambda)<1$ and the low M/Vd consists of the measurements with $M/Vd\times(1/\lambda)<0.7$. Overall, the results of this comparison show that the cracking indicator is reached first, as expected. For the shear indicators, the indicator based on the CSDT is reached generally before the indicator of the CSCT, and both indicators present similar values for the associated coefficient of variation. Generally, the stop criteria in the low M/Vd region are reached around 84% of the failure load, which would be too close to the critical load for application in proof load tests. However, the stop criteria in this region could serve as
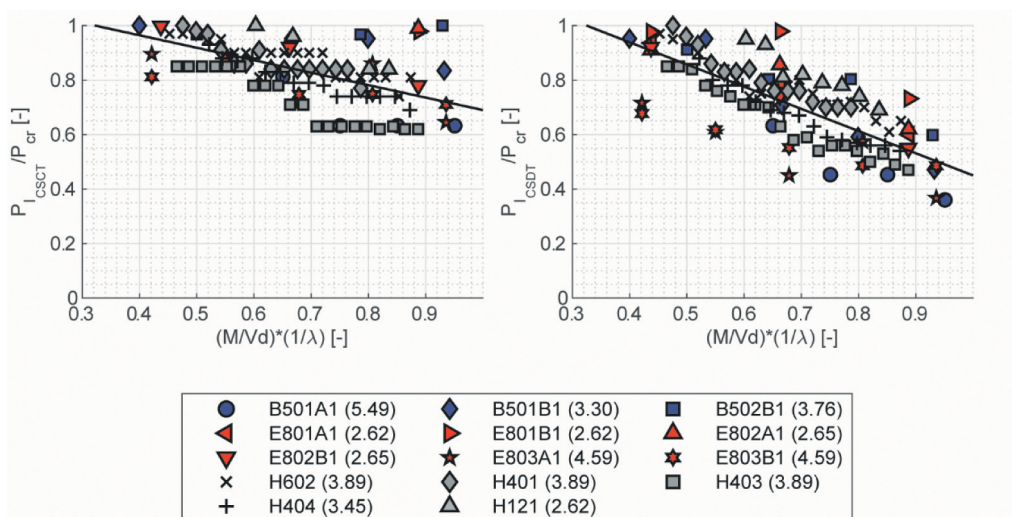
Figure 5. Results of the indicator based on the Critical Shear Crack theory and the Critical Shear Displacement Theory as a function of M/Vd normalized by factor λ.

warning signals for imminent failure. Overall, the proposed stop criteria are suitable for the reinforced concrete slab strips tested and they provide a different margin of safety as a function of the location along the shear span.

The Serviceability Limit State (SLS) crack width limit was, on average, reached at 51% of the failure load in the large M/Vd region, with a standard deviation of 0.11 and a coefficient of variation of 0.22. In the low M/Vd region, it was reached at an average of 74% of the failure load, with a standard deviation of 0.15 and a coefficient of variation of 0.21.

Table 2. Comparison between experiments and proposed stop criteria.

| | Large M/Vd | | | Low M/Vd | |
| | $0.8 < M/Vd \times (1/\lambda) < 1$ | | | $M/Vd \times (1/\lambda) < 0.7$ | |
	I_{CSDT}	I_{CSCT}	I_{CSDT}	I_{CSCT}
AVG	55%	77%	80%	88%
STD	0.10	0.13	0.12	0.08
COV	0.18	0.16	0.13	0.12

5 RECOMMENDATIONS FOR SHEAR STOP CRITERIA FOR SLAB STRIPS

To better understand the risk associated with reaching a stop criterion, the stop criteria are organized in a traffic light system, as also used by (Zhang, 2022). The system uses the following colors and interpretations: 1) green light corresponds to serviceability limit state and is related to cracking in the region close to the load l_{crm}, 2) yellow light corresponds to the ultimate limit state for shear and potential irreversible damage, and is related to the increase in the crack opening or the average longitudinal strain, as well as the opening of the critical shear crack in the low M/Vd region, and 3) red light corresponds to imminent failure for the ultimate limit state for shear, and is based on the indicator of increase in crack opening and the shear failure criteria from the theoretical shear models. It is recommended to monitor these regions using traditional measuring techniques such as LVDTs or 2D DIC to obtain measurements of crack widths or longitudinal strains. The recommended gauge length is 0.8d. Detailed information about the study of the optimal gauge length can be found on (Zarate Garnica

et al., 2022). These regions and the different levels of the stop criteria are also indicated in Figure 6.
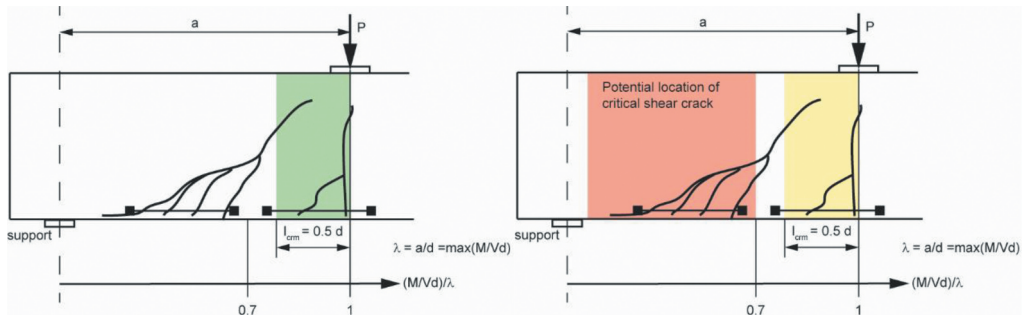

Figure 6.   Overview of stop light system for shear stop criteria for RC slab strips.

6   SUMMARY AND CONCLUSION

This paper shows the development of stop criteria for the ultimate limit state for shear and for the serviceability limit state for cracking from theoretical principles. These stop criteria are then compared to the experimental results from fourteen beams, and different critical regions in the shear span are identified. Finally, a traffic light system for the stop criteria is proposed.

From this research, the following conclusions can be drawn:

– A serviceability limit state cracking indicator can be used as a stop criterion in the region of the shear span close to the load to identify the beginning of flexural cracking.
– The two theoretically derived shear stop criteria, based on the Critical Shear Displacement Theory and the Critical Shear Crack Theory, perform equally well, with the stop criterion based on the CSDT generally being reached first.
– The shear stop criteria can be used to warn for imminent danger for collapse in the region corresponding to the lowest M/Vd.
– It is recommended to monitor the shear span using LVDTs or 2D DIC to obtain measurements of crack width or longitudinal strain.

ACKNOWLEDGMENT

REFERENCES

Alampalli, S., Frangopol, D. M., Grimson, J., Halling, M. W., Kosnik, D. E., Lantsoght, E. O. L., Yang, D., & Zhou, Y. E. (2021). Bridge Load Testing: State-of-the-Practice. *Journal of Bridge Engineering*, *26*(3), 03120002. https://doi.org/doi:10.1061/(ASCE)BE.1943-5592.0001678
CEN. (2005). Eurocode 2: Design of Concrete Structures - Part 1-1 General Rules and Rules for Buildings. NEN-EN 1992-1-1:2005. In (pp. 229). Brussels, Belgium: Comité Européen de Normalisation.
Gehri, N., Mata-Falcón, J., & Kaufmann, W. (2020). Automated crack detection and measurement based on digital image correlation. *Construction and Building Materials*, *256*, 119383.
Koekkoek, R. T., & Yang, Y. (2016). *Measurement Report on the transition between flexural and shear failure of RC beams without shear reinforcement*.

Lantsoght, E. O. (2023). Assessment of existing concrete bridges by load testing: barriers to code implementation and proposed solutions. *Structure and Infrastructure Engineering*, 1–13.

Lantsoght, E. O. L., Van der Veen, C., De Boer, A., & Hordijk, D. A. (2017). Proof load testing of reinforced concrete slab bridges in the Netherlands. *Structural Concrete*, *18*(4), 597–606.

Lantsoght, E. O. L., Van der Veen, C., & Hordijk, D. A. (2018). *Proposed stop criteria for proof load testing of concrete bridges and verification* IALCCE 2018, Ghent, Belgium.

Lantsoght, E. O. L., Van der Veen, C., Walraven, J., & De Boer, A. (2014). *Recommendations for the Shear Assessment of Reinforced Concrete Solid Slab Bridges* IABMAS 2014, Shanghai, China.

Lantsoght, E. O. L., Yang, Y., van der Veen, C., Hordijk, D. A., & de Boer, A. (2019). Stop Criteria for Flexure for Proof Load Testing of Reinforced Concrete Structures [Original Research]. *Frontiers in Built Environment*, *5*(47). https://doi.org/10.3389/fbuil.2019.00047

MatchID. (2022). *User manual*. https://www.matchid.eu/Software.html

Muttoni, A., & Fernández Ruiz, M. (2008). *Shear strength in one- and two-way slabs according to the Critical Shear Crack Theory* International FIB Symposium 2008, Amsterdam, The Netherlands.

The Mathworks, I. (2019). *Matlab R2019a, User's Guide*. In

Yang, Y. (2021). *Shear Capacity of RC Slab Structures with Low Reinforcement Ratio - an Experimental Approach* fib symposium 2021, Lisbon (online).

Yang, Y., Den Uijl, J. A., & Walraven, J. (2016). The Critical Shear Displacement theory: on the way to extending the scope of shear design and assessment for members without shear reinforcement. *Structural Concrete*, *17*(5), 790–798.

Yang, Y., Zárate Garnica, G., Lantsoght, E. O. L., & Hordijk, D. A. (2018). *Calibration of the shear stop criteria based on crack kinematics of reinforced concrete beams without shear reinforcement* fib conference 2018, Melbourne, Australia.

Zarate Garnica, G. I., de Vries, R., & Lantsoght, E. O. L. (2022). *Analysis report of reinforced concrete slabs for stop criteria*.

Zhang, F. (2022). *Acoustic emission-based indicators of shear failure of reinforced concrete structures without shear reinforcement* Delft University of Technology].